Light & Engineering
Vol. 27, No. 5, pp. 103–111, 2019 *https://doi.org/10.33383/2018-100*

ESTIMATION OF MEASUREMENT ERROR OF THE SEAWATER BEAM ATTENUATION COEFFICIENT IN TURBID WATER OF ARCTIC SEAS

Vladimir I. Burenkov, Sergei V. Sheberstov, Vladimir A. Artemiev, and Valery R. Taskaev

P.P. Shirshov Institute of Oceanology of the Russian Academy of Sciences, Moscow
E-mail: bur-07@yandex.ru

ABSTRACT

The article describes the estimation of measurement error of seawater beam attenuation coefficient using the Monte Carlo method. Measurements of the beam attenuation coefficient and its vertical distribution are the most common type of hydro-optical investigations since it is widely used for the research of light distribution in sea medium. Moreover, the beam attenuation coefficient is closely related to the concentration of the suspended substance and may be used for its estimation. Usually, the measurements of beam attenuation coefficient are conducted with small instrument base in rather transparent waters. In this case, the method errors of the beam attenuation coefficient measurement are low. However, in practice, cases of very turbid waters (near-bottom nepheloid layers), where measurement errors of beam attenuation coefficient significantly increase due to multiple scattering within the instrument base, are often encountered. The estimation of such errors is reviewed in this work. The effect of scattering phase function on the considered errors is described to the greatest extent. Moreover, the effect of the instrument base length and angle of view of the receiving system on measurement errors of beam attenuation coefficient is studied. Corresponding estimations are provided.

Keywords: beam attenuation coefficient, nepheloid layers, Monte Carlo method, measurement error, Bouguer law, multiple scattering

1. INTRODUCTION

Nowadays, the measurements of the beam attenuation coefficient c and its vertical distribution are the most widely used type of hydro-optical investigations. The value of the beam attenuation coefficient (alongside with other hydro-optical indicators) significantly affects the solar radiation (and radiation of artificial light sources) distribution in a water medium.

Numerous investigations have shown that the value of the beam attenuation coefficient is closely related to the concentration of the suspended substance and may be used for its estimation [1, 2]. It needs to be noted here that hydro-optical measurements have a particular advantage since they are conducted continuously in space and time, whereas geological methods are very time-consuming.

It should be noted that recently the measurements of beam attenuation coefficient are being widely used for the research of different biogeochemical processes in the ocean (among the recent publications, see, e.g. [3–5]).

The measurement method of beam attenuation coefficient is based on the Bouguer law $P = P_0e^{-cL}$, where P_0 and P are the values of radiant flux before and after the light passes the distance L in the water, c is the value of beam attenuation coefficient. For correct determination of c, it is necessary that the light beam coming out of the instrument had a low divergence and the receiving system had a low angle of view. In the rather transparent waters, the value of $\tau = cL$ is relatively low, but there are situations when it is essentially higher than one (e.g. in turbid waters in areas of river runoffs or in near-bottom nepheloid layers), and the multiple scattering of light along the beam axis is necessary to be taken into account in this case. This goal is the main subject of this work. It should be noted that the Monte Carlo method is applied for estimation of measurement error of beam attenuation coefficient for the first time.

2. PUM TRANSPARENCY METER. OPTICAL SCHEMATIC AND ADVANTAGES OF THE INSTRUMENT

Fig. 1 shows the optical schematic of the PUM transparency meter (universal small-size transparency meter) which is being used for field experiments of the Shirshov Institute of Oceanology, Russian Academy of Sciences recently [6].

The instrument is based on the classical two-channel optical arrangement with one light source and one photodetector, the reference channel is located inside the body. The main advantage of the two-channel arrangement is the elimination of non-stabilities of the light source and the photodetector in the course of measurement signal level setting on the basis of the reference one (which is required for calculation of beam attenuation coefficient).

In the measurement channel, the light source 1, which is a high-output LED, sends a light beam to the studied medium (seawater) through semi-transparent mirror 10, collimator 6, and illuminator 7. The beam reflected by cube-corner reflector 8 gets inside the instrument again through the illuminator 7, passes the lens 6 and, being reflected by the semi-transparent mirror 10, gets into the photodetector 2. In the reference channel, the light beam gets on the spherical mirror 3 through the semi-transparent mirror 10 and, being reflected by the former, through the same semi-transparent mirror, it gets to the photodetector, at output of which there is the interference filter 11 passing the radiation with light source wavelength (532 nm) and half-width of 20 nm.

For calculation of beam attenuation coefficient, two additional channels are used. The dark signal channel is required for calculation of background signal with the light source switched off and is used for compensation of the temperature drift of the photodetector (the background signal is subtracted from the reference signal). The reference channel is used for calculation of the background signal (the reference signal) from the light scattered by the water which gets into the measurement channel. The reference signal is measured with the light source switched off and is subtracted from the signal of the measurement channel. For additional reduction of external light, the narrow-band interference filter 11 with the same spectral characteristics as those of the light source is used. Formation and sequence of light fluxes to the input of the photodetector 2 are provided by the optical modulator 4 installed along the axis of the electric drive 5. Apart from closing the optical fluxes, the modulator forms synchronised impulses controlling switching on of the light source 1 and allowing to separate the components corresponding with light fluxes of each of the four channels out of the impulse signal in the photodetector output.

In the course of operation, the PUM transparency meter has undergone numerous retrofits. In particular, apart from the standard installation place of the cube-corner reflector at a distance of $L/2$ = 30 cm from the illuminator, installation of the cube-corner reflector is provided at a distance of $L/2$ = 5 cm for measurements in very turbid waters.

Main optical parameters of the PUM transparency meter are shown in Table 1.

Table 1. PUM Transparency Meter Parameters

Parameter	Value
Beam divergence	$2\cdot\theta_0 = 12'$ (in water)
Receiver view angle	$2\cdot\theta = 20'$
Beam width	$2w$=20 mm
Short base	L=10 cm
Long base	L= 60 cm
Collimator diameter	$2\cdot R$ = 35 mm

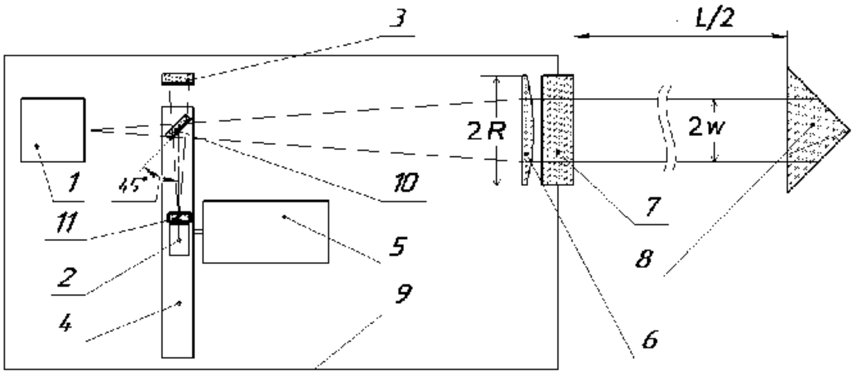

Fig. 1 Optical schematic of PUM transparency meter: 1 – light source; 2 – photodetector; 3 – spherical mirror; 4 – optical modulator; 5 – electric drive; 6 – collimator; 7 – illuminator; 8 – cube-corner reflector; 9 – sealed case of the instrument; 10 – semi-transparent mirror; 11 – interference filter

3. VERTICAL PROFILES MEASUREMENTS EXAMPLES OF BEAM ATTENUATION COEFFICIENT IN HIGH-TURBID WATERS

The measurements described below were conducted during the 69th expedition of the Research Vessel "Akademik Mstislav Keldysh" in 2017. The area of research was a wide one: from the Barents Sea to the East Siberian Sea.

The distribution of beam attenuation coefficient in the researched waters has high spatial-temporal variability. In this area, both waters with the value of *c* close to that of transparent ocean waters and high-turbid waters with the value of $\tau = c \times L$ essentially exceeding one are encountered. The locations of stations where anomalously high values of *c* ($c >$ 10 m^{-1}) are shown in Fig. 2.

Usually, such waters are encountered in near-bottom layers (the so-called near-bottom nepheloid layers caused by spreading of bottom sediments). In the Khatanga river mouth, the water is anomalously turbid ($c >$ 40 m^{-1}) from the surface to the bottom. The examples of the results of measurements conducted in such waters are shown in Fig. 3.

Fig. 3 shows that all the graphs have near-bottom nepheloid layers, where the values of beam attenuation coefficient *c* exceed 20 m^{-1} (in some cases, the value of *c* exceeded 50 m^{-1}). It is obvious that multiple scattering of light along the base

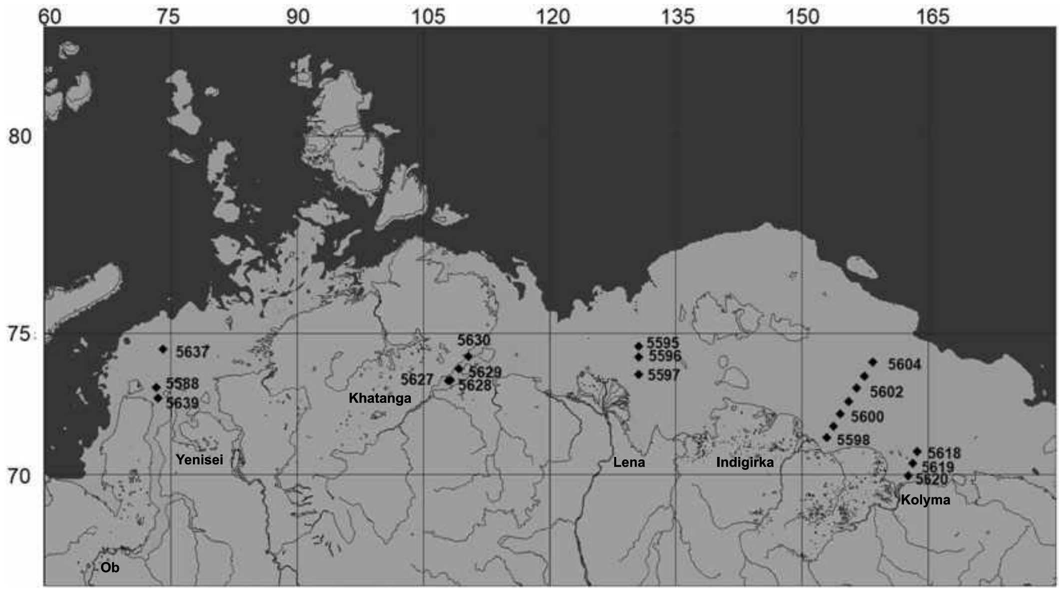

Fig. 2. Stations of the 69th expedition of the R/V "Akademik Mstislav Keldysh"

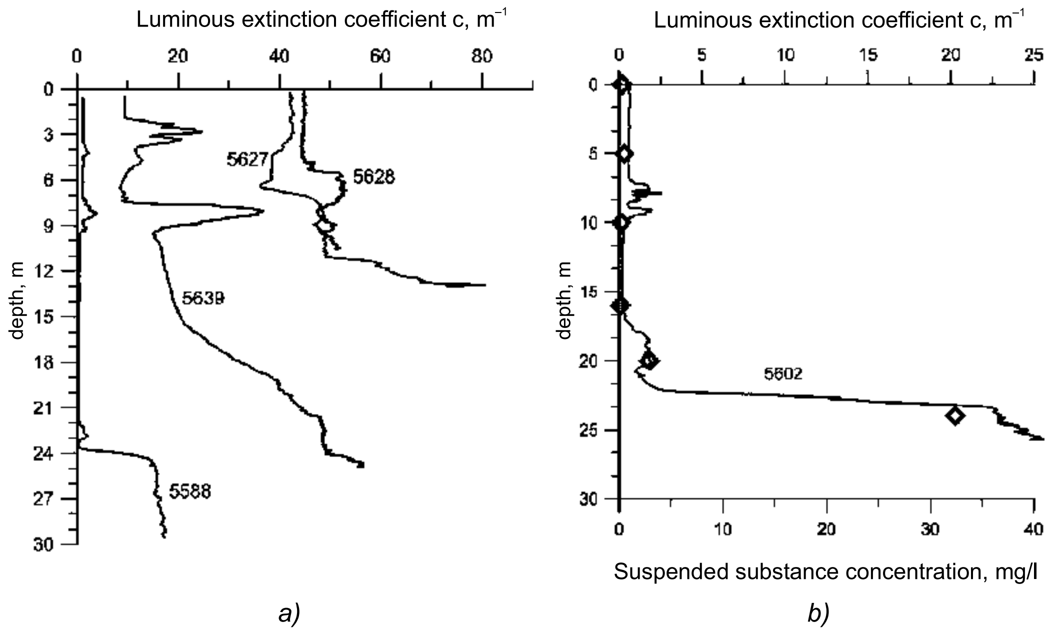

Fig. 3. Examples of Measurements of vertical profiles of beam attenuation coefficient in high-turbid waters. Station numbers are given in the graphs. a – st. 5627 and 5628 – Khatanga river mouth, st. 5588 and 5639 – Kara Sea; b – st. 5602 – East Siberian Sea in the area of the Indigirka river mouth. Diamonds indicate the suspended substance concentration. Thick near bottom nepheloid layer is well seen

length L should be taken into consideration for such layers. In all cases when the value of τ exceeded 9, the sensitivity of an instrument with long base was not sufficient, whereas the measurements with short base gave satisfactory results (Fig. 3).

The measurements of the vertical distribution of beam attenuation coefficient in near-bottom layers are well-confirmed by direct measurements of suspended substance concentration. The corresponding example is shown in Fig. 3b.

4. APPLICATION OF THE MONTE CARLO METHOD FOR ESTIMATION OF MEASUREMENT ERROR OF BEAM ATTENUATION COEFFICIENT

As a parameter of error estimation, the value $\delta c = c - c_{\text{meas}}$, where $c_{\text{meas}} = \ln(P_0/P)/L$ was selected. In [7], the problem of spreading of a narrow light beam, which essentially resolves itself into calculation of the value of P depending the parameters R, L, and optical properties of medium was considered. However, it is worth noting the difference between the setup of the problem and our case: the distribution of irradiance was studied at some distance from the source, i.e. the view angle of the receiver θ was equal to 90°, whereas in our case, θ = 10' and, as it will be explained below, this difference is quite essential.

The beam attenuation coefficient c measurement error caused by scattered light detection by the detector was calculated using the Monte Carlo method. The simplest variant of this method was used: direct modelling of photon trajectories [8, 9]. For each photon, the processes of absorption and scattering in medium, reflection from the cube-corner reflector, and return to the illuminator were modelled. Only those photons, for which the incidence angle did not exceed the value of θ, were taken into account.

First, let us consider the dependence of the calculation parameters on scattering phase function. Unlike the problems of remote sensing, in which the results are mostly defined by the behaviour of the phase function in the backward hemisphere, here the scattering at low angles of about 1° is the most essential factor which defines entry of the scattered light to the photodetector. Dependence of the results of calculations on scattering phase function, unlike other parameters considered below, which are known in advance or set a priori, is the most uncertain one. It is possible to use only reference data here.

The experimental data regarding scattering phase functions measured in the Indian Ocean at depths lower than 100 m and exceeding 100 m is contained in the Ocean Optics monograph, volume 1, part II,

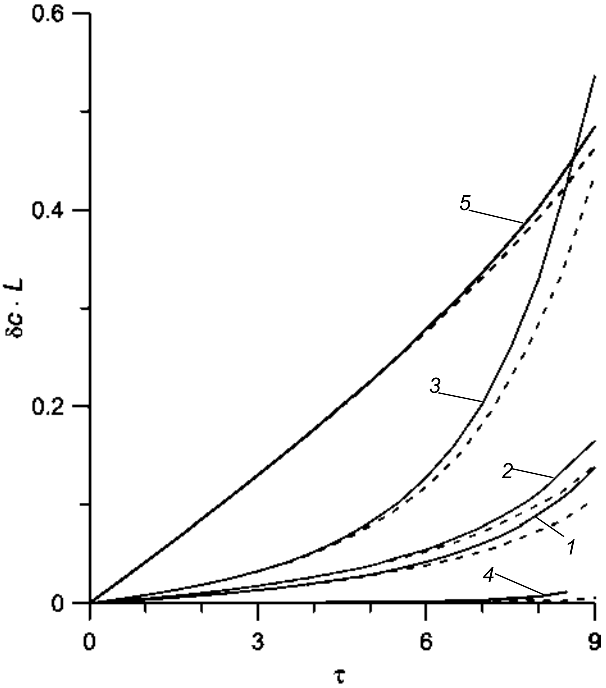

Fig. 4. Dependencies $\delta c{\cdot}L$ on optical thickness for different indicatrices: 1 – *ind1*, 2 – *ind2*; 3 – *Kl*, 4 – *Ks*, 5 – *Petzold*. Continuous lines – short base (0.1 m), dashed lines – long base (0.6 m)

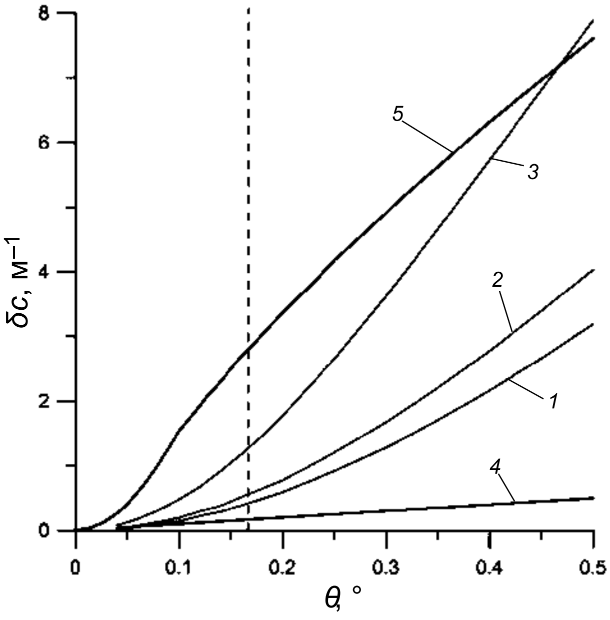

Fig. 5. Dependencies of δc on the receiver angle of view θ for different indicatrices: 1 – *ind1*, 2 – *ind2*; 3 – *Kl*, 4 – *Ks*, 5 – *Petzold*. Vertical dashed line indicates the value of the θ parameter for PUM

chapter 7 [10]. Below we will indicate these phase functions as *ind*1 and *ind*2 respectively.

Table 8.6 of the same monograph contains phase functions for pure water and for fine and coarse suspended substances. For coarse size (biogenic substance), the range of particle sizes was taken in the form of Junge distribution r^{-v}, where v =3. Refractive index of particles is equal to 1.03. For fine substance (terrigenous substance), complex distribution within the range of particle sizes from 0.01 to 1.3 mm was taken. In this case, the refractive index of particles is equal to 1.15. We will indicate scattering phase functions for coarse and fine fractions as *Kl* and *Ks* respectively.

In [11], the results of measurement of scattering phase function in coastal waters (San Diego bay) and in the waters of the open ocean within the range of angles from 0.1 to 175° are listed. This data is reproduced in [12] and at http://www.oceanoptics-book.info/view/references/publications.

If we presume that the only essential parameter with length dimension in this problem is the baseline length L, for the given phase function, the non-dimensional value $\delta c{\cdot}L$ depends only on the non-dimensional parameter $\tau = c{\cdot}L$. The graph of such dependence is shown in Fig. 4. It can be seen that, with relatively high values of the parameter τ, for some phase functions, for instance, for *Kl*, this presumption is not met: with the same value of the parameter τ, the value of $\delta c{\cdot}L$ for long base is less than for the short one. It is caused by the fact that, apart from L, there are other parameters with length dimension in the problem, in particular, the radius of the collimator R. Dependence of δc on R is essential with $R < L{\cdot}\tan\psi$, where ψ is the divergence angle of the photon beam with incidence angle less than the view angle of the receiver θ. The value of angle ψ essentially depends on the scattering phase function: the more the phase function is elongated forward, the less this angle is. With a short base, the condition $R > L{\cdot}\tan\psi$ is met for all phase functions, whereas with long base, it is not always so.

Dependencies of δc on the view angle of the receiver for different phase functions are shown in Fig. 5. For PUM, this angle equals to 0.167°. This dependence itself is rather obvious: the more the receiver view angle is as compared to the beam divergence, the higher is the effect of scattered light and the higher is the beam attenuation coefficient measurement error.

The conducted calculations show that changes in the value of beam divergence slightly affect the value of c measurement error (naturally if the beam divergence is significantly less than the receiver view angle). Moreover, the calculations show that changing the beam width slightly affects the results

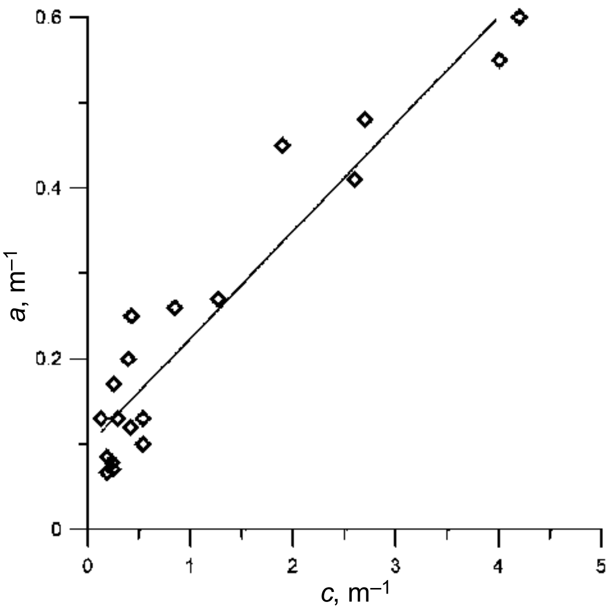

Fig. 6. Relation between the parameters of absorption and extinction in the Barents Sea (1998)

(if it is significantly less than the diameter of the illuminator).

It should be noted that the value of absorption, naturally, does not affect deviation from the Bouguer law. Its increase causes only a decrease of the relative measurement error of the beam attenuation coefficient.

5. ESTIMATION OF MEASUREMENT ERRORS OF THE BEAM ATTENUATION COEFFICIENT IN THE SURFACE LAYERS OF ARCTIC SEAS

Above, rather essential effect of scattering phase function in the low angles range on the beam attenuation coefficient was demonstrated. Below, we will consider the possibility of determination of the error of beam attenuation coefficient in the surface layer with scattering phase function taken into account. This possibility is based on the close relation between the backscattering coefficient

$$\int_{\frac{\pi}{2}}^{\pi} p(\gamma)\sin\gamma d\gamma \quad b_b = 2\pi \int_{\pi/2}^{\pi} \beta(\gamma)\sin(\gamma)d\gamma ,$$

where $\beta(\gamma)$ is the volume scattering function of sea water, and sub-surface radiance reflectance

$$\rho = \pi\cdot L_u/E_d,$$

where L_u is the sub-surface upwelling radiance, E_d is the sub-surface downwelling irradiance. The radiance reflectance ρ can be measured both by contact and remote (using satellite colour scanners) methods.

A simple and, at the same time, rather exact expression describing the dependence of the radiance reflectance on inherent optical properties is given in [13]: $\rho = 0.0922\cdot\pi\cdot b_b/a$, where a is the absorption coefficient of sea water, from which:

$$b_b = 3.45\rho a . \quad (1)$$

The relation between the absorption coefficient a and extinction coefficient c is acquired based on the results of measurements conducted in the Barents Sea in 1998 (the measurements were conducted both in turbid waters of Pechora Sea and in relatively transparent waters of the Western part of Barents Sea). At that time, diffuse attenuation coefficient K_d at a wavelength of 530 nm and the beam attenuation coefficient c were measured at the same time. According to [14], the relation between a and K_d is written as $K_d = D_0(\theta)\cdot k_1\cdot (a + b_b)$. Given that the measurements were conducted with the Sun zenith angle of about 60°, for approximate calculations, $D_0(\theta)\cdot k_1 = 1.3$ may be taken (see [14, table 4]). From here the value of $a(530)$ is determined (the value of b_b may be estimated based on the approximate formula $b_b = 0.018\cdot c/b$, where b is the seawater scattering coefficient [15]). The graph of dependence of the absorption coefficient on the extinction coefficient based on the measurements conducted in the Barents Sea in 1998 is given in Fig. 6. It can be seen that there is a rather close correlation between the considered parameters (determination coefficient $r^2 = 0.9$). The corresponding regression equation is written as a (530) = 0.0983· c (530) + 0.05, from which, with consideration of (1), we obtain:

$$b = 0.902c - 0.05, b_b = \rho\left(0.335c + 0.252\right). \quad (2)$$

For estimation of the scattering phase function, the two-parameter model of light-scattering properties of sea water [16] was used; in accordance with it, volume scattering function $\beta(\gamma)$ may be presented as the sum of contributions by pure sea water $\beta_w(\gamma)$ and fine and coarse suspended substances ($v_f\cdot\beta_f(\gamma)$ and $v_c\cdot\beta_c(\gamma)$ respectively):

$$\beta(\gamma) = \beta_w(\gamma) + v_f\beta_f(\gamma) + v_c\beta_c(\gamma), \quad (3)$$

where v_f and v_c are volume concentrations of fine and coarse suspended substances respectively; the tables of functions $\beta_w(\gamma)$, $\beta_f(\gamma)$, and $\beta_c(\gamma)$ for a wavelength of 550 nm are given in [10]. For recalculation to the operating wavelength of the transparency meter, we use the spectral dependence formulas: $\beta_w \sim \lambda^{-4,3}$, $\beta_f \sim \lambda^{-1,7}$, $\beta_c \sim \lambda^{-0,3}$.

To define the parameters of the model v_f and v_c, first, we integrate (3) over the whole sphere, then over the backward hemisphere. As a result, we obtain a pair of linear equations in two variables:

$$b=b_w+v_f b_f+v_c b_c;\ b_b=½b_w+v_f b_{bf}+v_c b_{bc}, \qquad (4)$$

where b_w is the scattering coefficient of pure sea water,

$$b_{f,c}=2\pi\int_0^{\pi}\beta_{f,c}(\gamma)\sin(\gamma)d\gamma,$$

$$b_{b_{f,c}}=2\pi\int_{\pi/2}^{\pi}\beta_{f,c}(\gamma)\sin(\gamma)d\gamma.$$

Solving the equations (4) with consideration of (1) and (2), applying the parameters v_f *and* v_c to (3), and multiplying the result by the normalization factor $1/b$, we obtain the scattering phase function, and therefore, all parameters required for calculation using the Monte Carlo method.

In Fig. 7, the estimation results of the dependence of the extinction coefficient measurement error caused by multiple scattering on radiance reflectance for different values of L and c are shown. Like in Fig. 4, the difference of the values of the non-dimensional value $\delta c{\cdot}L$ for similar values of τ but different values of L is caused by the fact that, with long base, the value $L{\cdot}\tan\psi$ (ψ is the angle of light beam divergence) exceeds the collimator radius.

Estimation of the measurement error of the extinction coefficient c using the parameter ρ is possible only for surface layers. Possible values of the parameter ρ for this region may be evaluated based on satellite data or data of contact measurements, e.g. by means of a floating spectroradiometer [17]. During the 69th cruise of the R/V "Akademik Mstislav Keldysh", the highly turbid surface layers we were interested in were found at stations 5627 and 5628 in the Khatanga river mouth (Fig. 2, 3). Shipboard measurements of ρ were not conducted at these stations. The estimation capability of this parameter by means of satellite data is considered below.

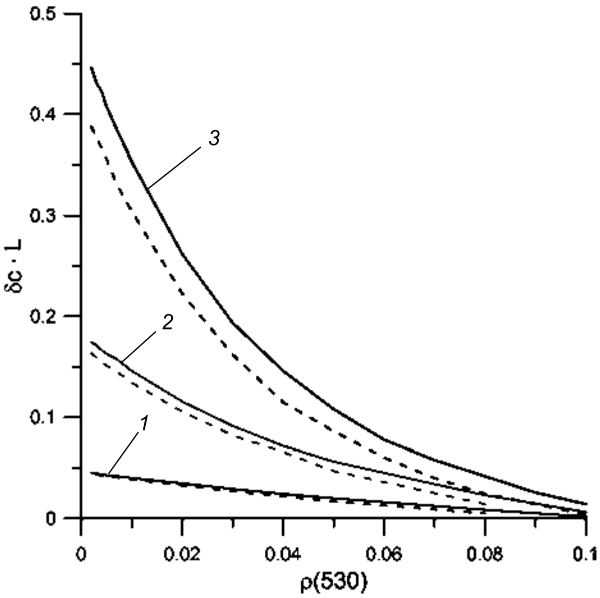

Fig. 7. Dependence of measurement error of the luminous extinction coefficient caused by multiple scattering on luminance factor of water medium: 1 – $\tau = 3$; 2 – $\tau = 6$; 3 – $\tau = 8$. Continuous lines – $L = 0.1$ m, dashed lines – $L = 0.6$ m

The data files of the *MODIS Aqua* and *MODIS Terra* satellite ocean colour scanners contain the parameter $R_{rs}(\lambda) = L_u^+/E_d^+$ (L_u^+ is the water-leaving radiance, E_d^+ is the downward irradiance above the surface) for a wavelength of $\lambda = 531$ nm. The value ρ can be with a good accuracy calculated using the formula $\rho(\lambda) = R_{rs}(\lambda)/(0.495{\cdot}R_{rs}(\lambda) + 0.165)$ [18]. There are no data exactly referenced to coordinates and measurement time of stations 5627 and 5628, however, it can be proposed that the required value of ρ lies within the interval between the minimal and the maximum values of it for this region within a month. Based on the *MODIS Aqua* data, average values of ρ for each day of August, 2017 were calculated within the inner part of the contour bounding the Khatanga river mouth (in September, the data for this region was not available due to overcast conditions). Average value was equal to 0.044, maximum value was equal to 0.069, and minimal one was equal to 0.017. From the data shown in Fig. 7 follows that, in case of using a short base L=0.1 m with minimal value of ρ, the relative measurement error of the extinction coefficient is 4 % for $c = 80$ m^{-1} and 2 % for $c = 20$ m^{-1}.

CONCLUSION

The value of scattering phase function rather essentially affects the measurement error of the extinction coefficient (the more the phase function is prolonged, the higher is the error). Note that it relates to scattering at angles of about 1°. During measurements in surface layers, for estimation of the scattering phase function, the value of radiance reflectance at a wavelength of 530 nm ρ (530) may be used. In this case, the measurement error of c is low when the contribution of the coarse suspended substance in scattering at small angles is insignificant (the values of ρ (530) are rather high). In case, when the coarse suspended substance prevails in small-angle scattering, the considered error significantly rises (the values of ρ (530) are rather low). During measurement of the extinction coefficient in deep layers (in particular, in the near-bottom nepheloid layer), naturally, there are no phase function data, and the data given in [10] should be used for estimation of the measurement error of the extinction coefficient.

The instrument base length significantly affects the measurement error of c with high optical thicknesses of $\tau = c \cdot L$ (up to a few tens of a percent). Therefore, for measurement of the extinction coefficient in turbid waters, it is necessary to use short base for which the measurement errors of c caused by multiple scattering along the base length are significantly lowered.

The conducted calculations show that the receiver view angle significantly affects the measurement error of c. Therefore, it is necessary to use instruments with beam divergence significantly lower than the view angle of the receiver. Moreover, the calculations show that changing of the beam width slightly affects the results (naturally, if the beam radius is significantly less than the radius of the input hole of the receiver).

The results of measurements described herein and the conducted calculations confirm that the PUM transparency meter with short base may be recommended for measurement of the beam attenuation coefficient in highly turbid waters.

ACKNOWLEDGMENT

This research was performed in the framework of the state assignment of Minobrnauki RF (theme No.0149–2019–0003). The authors are grateful to O.V. Kopelevich for attention to the work and valuable comments. The authors thank M.D. Kravchishina for provided suspended substance concentration data.

REFERENCES

1. Burenkov V.I., Kuptsov V.M., Sivkov V.V., Shevchenko V.P. Prostranstvennoe raspredelenie i dispersnyi sostav vzvesi v more Laptevykh v avguste-sentiabre 1991 [Spatial Distribution and Disperse Composition of Suspended Substance in the Laptev Sea in August-September, 1991] // Okeanologiia, 1997, Vol. 37, No. 6, pp. 920–927.

2. Lisitsyn A.P., Shevchenko V.P., Burenkov V.I. Gidrooptika i vzves arkticheskikh morei [Hydrooptics and Suspended Substance of Arctic Seas] // Optika atmosfery i okeana, 2000, Vol. 13, No. 1, pp. 71–79.

3. Ramírez-Pérez M., Rüdiger R., Torrecilla E., Piera J. Cost-Effective Hyperspectral Transmissometers for oceanographic Applications: Performance Analysis // Sensors, 2015, Vol. 15, pp. 20967–20989. DOI:10.3390/s150920967.

4. Moore C., Barnard A., Fietzek P., Lewis M.R., Sosik H.M., White S., Zielinski O. Optical tools for ocean monitoring and research // Ocean Sci., 2009, Vol. 5, pp. 661–684.

5. Kopelevich Oleg V. Use of Light in the Exploration and Research of the Seas and Oceans// Light & Engineering Journal, 2017, Vol.25, #4, pp. 4-17.

6. Artemiev V.A., Taskaev V.R., Burenkov V.I., Grigoriev A.V. A multi-purpose compact transmissometer // Proc. of the III Int. Conf. “Current Problems in Optics of Natural Waters” – ONW’2005, St. Petersburg, Russia, 2005.

7. Dolin L.S., Saveliev V.A. Novaia model razmytiia svetovogo puchka v srede s silno anizotropnym rasseianiem [New Model for the Light Beam Spread Function in a Medium with Strongly Anisotropic Scattering] // Bulletin of AS, atmopsheric and oceanic physics, 2000, Vol. 36, No.6, pp. 794–801.

8. Ermakov S.M., Mikhailov G.A. Statisticheskoe modelirovanie [Statistical Modelling] // Nauka, Moscow, 1982, 296 p.

9. Kargin B.A. Statisticheskoe modelirovanie polia solnechnoi radiatsii v atmosfere [Statistical Modelling of Solar Radiation Field in Atmosphere] // VC SO AN USSR, Novosibirsk, 1984, 206 p.

10. Kopelevich O.V. Maloparametricheskaia model opticheskikh svoistv morskoi vody [Few-parameter Mod-

el of Optical Properties of Sea Water] // Nauka, Moscow, 1983, Vol. 1, pp. 208–234.

11. Petzold T.J. Volume scattering functions for selected ocean waters // Scripts Inst. Oceanogr. Report SIO, 1972, pp. 72–78.

12. Mobley C.D. Light and water. Radiative transfer in natural waters // Academic Press, 1994.

13. Morel A., Gentili B. Diffuse reflectance of oceanic waters. Bidirectional aspects // Appl. Optics, 1993, Vol. 32, pp. 6864–6879.

14. Gordon H.R. Can the Lambert-Beer Law be applied to the diffuse attenuation coefficient of ocean water // Limnol., Oceanogr., 1989, Vol. 35, No. 8, pp. 1389–1409.

15. Levin I.M. Relation between the seawater optical properties at 550 nm: estimate of its accuracy and extension to case 1 waters // Proc. of the III Int. Conf. "Current Problems in Optics of Natural Waters" – ONW'2005, St. Petersburg, Russia, 2005.

16. Kopelevich O.V., Gushchin O.A. O statisticheskikh i fizicheskikh modeliakh svetorasseivaiushchikh svoistv morskoi vody [On Statistical and Physical Models of Light Scattering Properties of Sea Water] // Bulletin of AS USSR, Atmospheric and Oceanic Physics, 1983, Vol. 14, No. 9, pp. 967–973.

17. Artemiev V.A., Burenkov V.I., Vortman M.I., Grogoriev A.V., Kopelevich O.V., Khrapko A.N. Podsputnikovye izmereniia tsveta okeana novyi plavaiushchii spektroradiometr i ego metrologiia [Sea Truth Measurements of Ocean Colour: New Floating Spectroradiometer and its Metrology] // Oceanology, 2000, Vol. 40, No. 1, pp. 148–155.

18. Lee Z., Carder K.L., Mobley C.D., Steward R.G., Patch J.S. Hyperspectral remote sensing for shallow waters. I. A semianalytical model // Applied Optics, 1998, Vol. 37, No. 27, pp. 6329–6338.

Vladimir I. Burenkov,
Ph.D. in Physical and Mathematical Sciences (1975). Graduated from MIPT (1970). Leading scientific worker of IO RAS

Vladimir A. Artemiev,
graduated from the Radiotechnical department of Moscow Aviation Institute (1973). Senior scientific worker of IO RAS

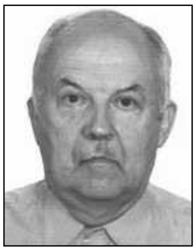

Sergei V. Sheberstov,
graduated from the Mechanical and Mathematical Department of Moscow State University (1967). Senior scientific worker of IO RAS

***Valery R. Taskaev*,**
Graduated from the Physical Department of Moscow State University (1980). Leading engineer of IO RAS